Human phosphatase CDC14A regulates actin organization through dephosphorylation of epithelial protein lost in neoplasm

Nan-Peng Chen[a,b], Borhan Uddin[a,b], Robert Hardt[a], Wen Ding[a], Marko Panic[a,b], Ilaria Lucibello[a], Patricia Kammerer[c], Thomas Ruppert[a], and Elmar Schiebel[a,1]

[a]Zentrum für Molekulare Biologie der Universität Heidelberg (ZMBH), Deutsches Krebsforschungszentrum (DKFZ)–ZMBH Allianz, Universität Heidelberg, 69120 Heidelberg, Germany; [b]Hartmut Hoffmann-Berling International Graduate School of Molecular and Cellular Biology (HBIGS), Universität Heidelberg, 69120 Heidelberg, Germany; and [c]Max Planck Institute of Biochemistry, 82152 Martinsried, Germany

Edited by Thomas D. Pollard, Yale University, New Haven, CT, and approved April 11, 2017 (received for review November 24, 2016)

CDC14 is an essential dual-specificity phosphatase that counteracts CDK1 activity during anaphase to promote mitotic exit in *Saccharomyces cerevisiae*. Surprisingly, human CDC14A is not essential for cell cycle progression. Instead, it regulates cell migration and cell adhesion. Little is known about the substrates of hCDC14A and the counteracting kinases. Here, we combine phospho-proteome profiling and proximity-dependent biotin identification to identify hCDC14A substrates. Among these targets were actin regulators, including the tumor suppressor eplin. hCDC14A counteracts EGF-induced rearrangements of actin cytoskeleton by dephosphorylating eplin at two known extracellular signal-regulated kinase sites, serine 362 and 604. hCDC14A^{PD} and eplin knockout cell lines exhibited down-regulation of E-cadherin and a reduction in α/β-catenin at cell–cell adhesions. Reduction in the levels of *hCDC14A* and *eplin* mRNA is frequently associated with colorectal carcinoma and is correlated with poor prognosis. We therefore propose that eplin dephosphorylation by hCDC14A reduces actin dynamics to restrict tumor malignancy.

CDC14 | eplin | actin dynamics

The highly dynamic nature of the actin network of nonmuscle cells contributes to its functions in cell migration, cell synaptic transmission, endocytosis, and the immune response (1–3). It is therefore not surprising that deregulation of actin is associated with a range of human diseases, including leukemia, kidney disorders, and cancer development (4, 5). Long lists of actin-associated proteins from Rho GTPases, kinases, phosphatases, and actin-binding proteins regulate actin filament dynamics (1, 3, 4, 6–8). Actin-bundling proteins such as α-actinin, fascin, and filamin cross-link actin filaments into bundles and play important roles in regulating membrane protrusions and cell mobility (9–13). Cofilin severs existing actin filaments to generate more free ends and thus plays a critical role in actin dynamics (9, 10, 14, 15). The protein epithelial protein lost in neoplasm (eplin) bundles F-actin filaments and can control G-actin nucleation by regulating the activity of the Arp2/3 actin complex (16). Interestingly, the activity of eplin is regulated through phosphorylation by extracellular signal-regulated kinase (ERK) at serine residues 362 and 604 (17). However, the phosphatase that reverses these important phosphorylations is unknown.

In *Saccharomyces cerevisiae,* the dual-specificity phosphatase CDC14 counteracts cyclin-dependent kinase (Cdk1) activity to drive mitotic exit (18, 19). Therefore, *CDC14* is essential for the viability of *S. cerevisiae*. In contrast, its ortholog, *CDC14A*, is not essential for the viability of either human or chicken DT40 cells. Surprisingly, cells in which the *hCDC14A* coding sequence had been disrupted did not show any obvious defects in cell cycle progression (18, 19). However, we recently reported that hCDC14A colocalizes with F-actin at the leading edge of cells and stress fibers where it regulates actin dynamics. This regulation is important for cell migration and cell adhesion (20).

Because there have been no systematic attempts to identify phospho-sites that are regulated by hCDC14A, we know relatively little about the identity of either the proteins that are dephosphorylated by hCDC14A or, indeed, the kinases that counteract hCDC14A in human cells. The only known substrate of hCDC14A that acts within the actin cytoskeleton is the protein Kibra (20, 21). However, considering the broad distribution of hCDC14A throughout the actin network, it is highly likely that hCDC14A dephosphorylates additional actin-associated proteins.

To identify hCDC14A substrates and decipher the molecular mechanisms by which hCDC14A controls cell migration, we combined phospho-proteome analysis with the biotin identification (BioID) proximity assay (22). These approaches identified the potent tumor suppressor eplin as a key actin-associated hCDC14A substrate. We show that hCDC14A controls actin-bundling activity of eplin to locally modulate actin rearrangements by counteracting EGF-induced ERK-mediated phosphorylation of eplin. Eplin also links F-actin to the E-cadherin–α/β catenin complex (23). Consistently, we found a reduction in the enrichment of α/β catenin at cell–cell junctions and decreased E-cadherin levels when either hCDC14A phosphatase activity was ablated or eplin was removed. This striking correlation indicates that hyperphosphorylated eplin lacks the ability to interconnect the E-cadherin–α/β catenin complex with F-actin. As down-regulation of *hCDC14A* and *eplin* is a common feature of colorectal cancer and is associated with poor prognosis, our data strongly suggest that loss of hCDC14A–eplin

Significance

Human hCDC14A phosphatase has been shown to regulate cell migration and adhesion by modulating actin dynamics. Here we identify the potent tumor suppressor eplin as an hCDC14A substrate. Through dephosphorylation of serine residues 362 and 604 of eplin, hCDC14A promotes F-actin bundling and counteracts EGF-induced membrane ruffling. Cells lacking hCDC14A activity or eplin expression showed reduced E-cadherin levels and β-catenin retention at cell–cell junctions and formed more invasive colonies than wild-type cells. Expression of a phospho-inhibitory, but not a phospho-mimetic, *eplin* mutant rescued these phenotypes. Database analysis indicated that hCDC14A and eplin are frequently inactivated in human colorectal cancer and this is associated with poor prognosis. Therefore, the hCDC14A and eplin axis plays an important role in limiting tumor malignancy.

Author contributions: N.-P.C. and E.S. designed research; N.-P.C., B.U., R.H., W.D., M.P., I.L., and P.K. performed research; T.R. contributed new reagents/analytic tools; N.-P.C., B.U., R.H., and W.D. analyzed data; and N.-P.C. and E.S. wrote the paper.

The authors declare no conflict of interest.

This article is a PNAS Direct Submission.

[1]To whom correspondence should be addressed. Email: e.schiebel@zmbh.uni-heidelberg.de.

This article contains supporting information online at www.pnas.org/lookup/suppl/doi:10.1073/pnas.1619356114/-/DCSupplemental.

regulation may be a key step in driving the malignancy of invasive colorectal cancers.

Results

Phospho-Proteome Analysis Revealed Multiple Actin Regulators as hCDC14A Substrates. We applied affinity purification of phospho-peptides followed by large-scale phospho-proteomics to identify hCDC14A substrates. HeLaTet$_{ON}$-*hCDC14A-YFP* and Tet$_{ON}$-*YFP* cells [stable integration into the flippase recognition target (FRT) site] were grown in heavy ($Arg^{13}C^{15}N$ $Lys^{13}C^{15}N$) and light ($Arg^{12}C^{14}N$ $Lys^{12}C^{14}N$) medium, respectively (Fig. 1*A*). After eight passages, addition of doxycycline (Dox) to the medium induced *hCDC14A-YFP* and *YFP* expression. Twenty-four hours later, proteins were extracted, the extracts were mixed at a ratio of 1:1, and, after phospho-peptide enrichment, peptides were analyzed by LC-MS/MS. Over 14,000 phospho-sites were identified in each of three independent replicate experiments. Surprisingly, only 68 phospho-sites (0.5%) belonging to 51 proteins (threshold = 0.5) were hypo-phosphorylated upon *hCDC14A-YFP* expression compared with the *YFP* control (Fig. 1*B* and Table S1). Of the 68 hypo-phosphorylated peptides, 65 (95.6%) contained phospho-serine (P-serine) residues and only 3 (4.4%) phospho-threonine (P-threonine), whereas P-serine represented 80.6% and P-threonine 18.6% of the global phospho-proteome of these cells. Thus, in line with in vitro data, in vivo hCDC14A also appears to preferentially target P-serine residues (24, 25).

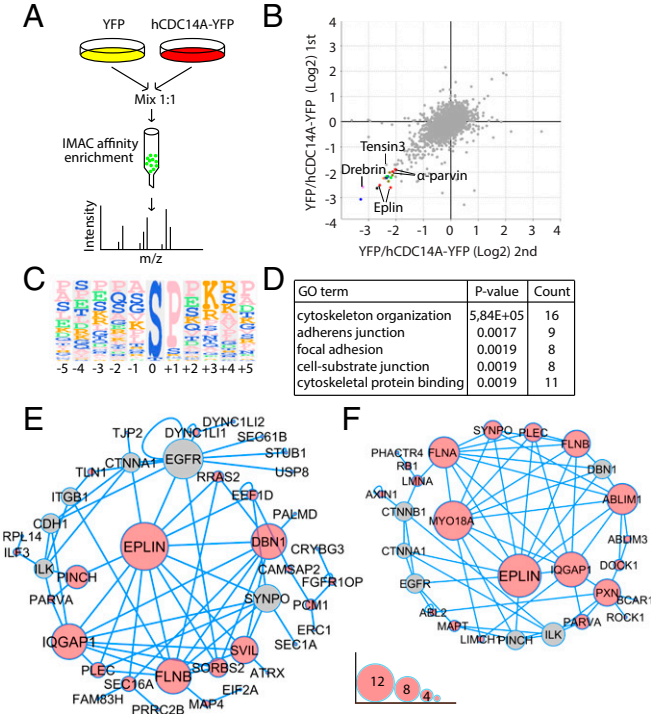

Fig. 1. (*A*) HeLa hCDC14A-YFP and HeLa YFP-inducible stable cell lines were labeled with heavy ($Arg^{13}C^{15}N$ $Lys^{13}C^{15}N$) and light ($Arg^{12}C^{14}N$ $Lys^{12}C^{14}N$) medium, respectively. Phospho-peptides were enriched and then applied on LTQ-Orbitrap for LC-MS/MS analysis. (*B*) Scatter plot of two replicate LC-MS/MS experiments. (*C*) Peptides of *B* that were hypo-phosphorylated at least twofold were included in this analysis. (*D*) Top five GO protein classifications based on cellular components are shown with *P* values and protein counts. (*E*) Molecular network based on the hypo-phosphorylated proteins upon *hCDC14A* overexpression. (*F*) Molecular network based on the hyper-phosphorylated proteins in *hCDC14A*^{KO} *hCDC14B*^{KO} cells. Only pSP/pTP sites were considered in this analysis. Protein–protein interactions among the hits were extracted from STRING and BioGrid and then integrated using Cytoscape. The size of the circle represents the number of interactors. IMAC, immobilized metal affinity chromatography.

Hypo-phosphorylated peptides were analyzed with the Perseus program to generate a consensus dephosphorylation motif for hCDC14A (Fig. 1*C*). This analysis is consistent with structural data (26) indicating that hCDC14A shares a common preference with cyclin-dependent kinases in being proline directed with a preference for lysine or arginine three residues after the phosphorylation site (25). The presence of proline residues at positions -1, -2, and +2 indicates that hCDC14A may also counteract other kinases such as ERK1/2 and glycogen synthase kinase 3 (GSK-3β) that emulate cyclin-dependent kinases in being proline-directed kinases yet have a preference for additional proline residues surrounding the phosphorylation site (www.phosphosite.org/). Consistent with hCDC14A's localization and function along F-actin, gene ontology enrichment revealed that the majority of hCDC14A substrates were either involved in the organization of the actin cytoskeleton or associated with adherens junctions and focal adhesion sites (Fig. 1*D*). Bioinformatic analysis using STRING and BioGrid revealed a molecular network of multiple actin regulators (Fig. 1*E*) that contained a high number of actin-bundling proteins such as eplin, drebrin, filamin, and supervillin.

To validate the data arising from the transient *hCDC14A* overexpression approach, we compared the phospho-proteomes of wild-type (WT) and *hCDC14A hCDC14B* double knockout (*hCDC14A/B*-KO) RPE1 cells. We used *hCDC14A*$^{\Delta/\Delta}$ *hCDC14B*$^{\Delta/flox}$ cell lines acutely infected with AdCre for this experiment (*hCDC14A/B*-KO) to minimize adaptation in response to the absence of the *hCDC14B* gene. Forty-nine cytoskeletal proteins were hyper-phosphorylated in comparisons between the *hCDC14A/B*-KO and WT cells. However, in contrast to the *hCDC14A* overexpression screen, in which the vast majority of dephosphorylated sites were "pSP/pTP" (Fig. 1*C*; 84.1%), only 60% of hyper-phosphorylated sites of the *hCDC14A/B*-KO screen were pSP/pTP. The remaining sites were not flanked by a proline residue and so probably arose from adaptation to the consequences of the prolonged lack of hCDC14A activity, for example, as a secondary consequence of the long-term down-regulation of other phosphatase(s) or up-regulation of kinase (s). Of the pSP/pTP substrates, the spectrum of the interaction network of hyper-phosphorylated cytoskeletal proteins of *hCDC14-KO* cells was reminiscent of the hypo-phosphorylated proteins of Tet$_{On}$-*hCDC14A* cells in being focused around eplin (Fig. 1 *E* and *F* and Table S2). Given that hCDC14A associates with the actin cytoskeleton (20) and that hCDC14B is enriched in the nucleus during interphase before associating with the mitotic chromatin (Fig. S1*A*), the lack of hCDC14A activity is probably responsible for the hyper-phosphorylation of actin-associated proteins in the RPE1 *hCDC14A/B*-KO cells.

hCDC14A Interaction Network by BioID. One of the challenges for the identification of hCDC14A substrates is the transient nature of the interaction between the phosphatase and its substrate (27, 28). The BioID approach is therefore highly attractive for this task as it is able to identify weakly interacting proteins because it supports efficient enrichment by virtue of the fact that neighbors are identified as a result of their biotinylation by hyperactive promiscuous biotin ligase BirA that has been fused to the protein of interest (22). To confirm hCDC14A substrates, we performed a proximity interactor screen with hCDC14A-BirA-HA as bait (Fig. 2*A*). Tet$_{ON}$-*hCDC14A-BirA-HA* and Tet$_{ON}$-*BirA-HA* cells were analyzed following the experimental stable isotope labeling with amino acids in cell culture (SILAC) approach outlined in Fig. 1*A*. The biotinylation reaction was initiated by the addition of biotin at the same time as the Tet$_{ON}$ promoter was induced by doxycycline. After affinity purification of biotinylated proteins and mass spectrometric analysis, 46 proteins were significantly more biotinylated in the *hCDC14A-BirA-HA* cells than in the *BirA-HA* control (Fig. S1*B*; threshold = 2). Gene Ontology (GO) analysis of partners revealed an enrichment of proteins with functions in exosome formation at focal adhesion and cell junction sites (Fig. S1*C* and Table S3). The

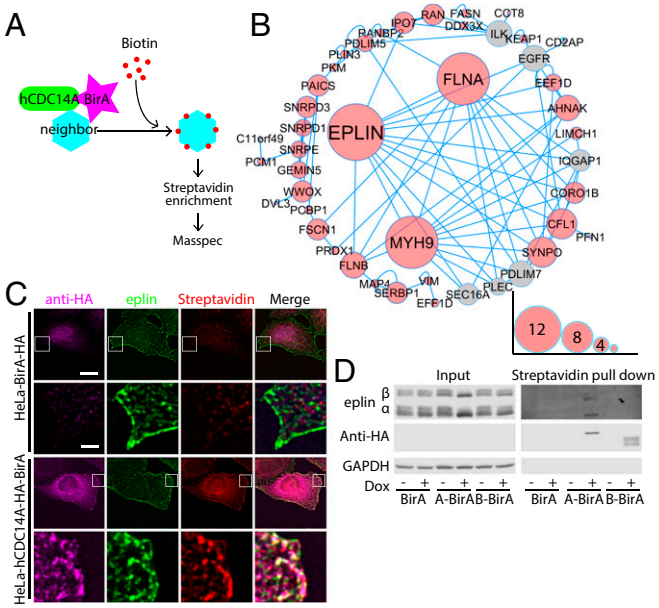

Fig. 2. (*A*) Scheme for BioID experiment. (*B*) Molecular network based on the interactors/neighbors identified in the BioID. (*C*) Eplin colocalizes with hCDC14A and biotinylation signals at the cell edge. (Scale bars: *First* row, 10 μm; *Second* row, 2 μm.) (*D*) Streptavidin pull-down experiment showed that eplin from hCDC14A-BirA-HA cell lysate was biotinylated. Note, doxycycline-induced expression of *hCDC14A-BirA-HA* and *hCDC14B-BirA-HA* was not detectable at the loaded protein amount in the input.

Kibra paralogue WWC2 was identified in the hCDC14A BioID (Table S3). The actin bundler eplin once again occupied a pivotal position in the hCDC14A interaction network (Fig. 2*B*).

Because eplin plays a crucial role in the regulation of actin dynamics and cell transformation, we focused upon understanding the relationship between eplin and hCDC14A. Eplin is expressed as two isoforms, α- and β-eplin, which have translation starts in exons 4 and 2, respectively (29) (Fig. S2 *A* and *B*). The actin-bundling activity of both eplin isoforms depends on the centrally localized LIM domain (exons 10–11) and two flanking regions (16, 29). Both isoforms contain the two previously characterized ERK phosphorylation sites at positions 362 and 604 (numbering refers to β-eplin). We began by monitoring the localization and biotinylation status of eplin in the *hCDC14A-BirA-HA* and *BirA-HA* cells. Eplin colocalized with hCDC14A-BirA-HA and the streptavidin signal at the cell leading edge (Fig. 2*C*), a colocalization that was absent from *BirA-HA* cells (Fig. 2*C*). Enrichment of biotinylated proteins by streptavidin pull-down showed that both isoforms of eplin were biotinylated in *hCDC14A-BirA-HA* but not in *hCDC14B-BirA-HA* or *BirA-HA* cell lysates, confirming the specificity of the interaction between hCDC14A and eplin (Fig. 2*D*). Moreover, the mobility of the upper band of α- and β-eplin increased upon *hCDC14A-BirA-HA* expression (Fig. 2*D*, lane 4), which is suggestive of an hCDC14A-dependent dephosphorylation of both eplin isoforms.

Together, the hCDC14A phospho-proteome and BioID analyses define an interaction network of hCDC14A with the actin-bundling protein eplin at its heart.

hCDC14A Dephosphorylates Eplin. Next, we verified the interaction between eplin and hCDC14A by coimmunoprecipitation. We cotransfected *flag-β-eplin* and *myc-hCDC14A* in HEK293T cells and performed immunoprecipitation experiments. The phosphatase dead mutant (C278S) version of hCDC14A but not the WT hCDC14A or GFP was coimmunoprecipitated by flag-β-eplin (Fig. 3*A*). This preferential association of the mutant hCDC14A protein with eplin is consistent with the previous demonstration that CDC14^{C278S} functions as a substrate trap that binds substrates tighter than the WT CDC14 (27). Thus, eplin and hCDC14A are present in common complexes.

Expression of *hCDC14A* in HeLa cells prompts the dephosphorylation of serine residues 362, 374, 604, and 609 of both isoforms of eplin (Fig. 1). These residues are conserved throughout mammals (Fig. S3*A*). To further confirm that these sites in eplin are regulated by hCDC14A in vivo, HEK293T cells were transfected with *flag-β-eplin* without (mock) or with *myc-hCDC14A*. Mass spectrometric analysis of the immunoprecipitated flag-β-eplin showed that phosphorylation of all four serine residues was strongly reduced by the expression of *myc-hCDC14A* (Fig. S3*B*). Thus, hCDC14A has the ability to dephosphorylate serine residues 362, 374, 604, and 609 of eplin in cells.

EGF treatment of cells activates ERK, which in turn phosphorylates α- and β-eplin at two serine residues at positions 362 and 604 (17, 30). Because both ERK sites were identified in the hCDC14A phospho-proteomic analysis (Fig. 1 and Fig. S3*B*), we asked whether hCDC14A could antagonize ERK phosphorylation of eplin. In logarithmically growing HeLa cells, both eplin isoforms were resolved as multiple bands in immunoblots. Expression of *hCDC14A* increased the migration of α- and β-eplin (Fig. 3*B*, lane 3), reflecting a reduction in phosphorylation of eplin. This dephosphorylation was not observed when the phosphatase dead *hCDC14*^{C278S} was expressed (Fig. 3*B*, lane 7). EGF treatment invoked a reduction in the migration of α- and β-eplin (Fig. 3*B*, lanes 2 and 6). However, when cells were treated with EGF after *hCDC14A* induction, α- and β-eplin migrated at an intermediate position in between the hyper- and hypo-phosphorylated forms, indicating that there was an antagonistic impact of hCDC14A on the ERK phosphorylation events on eplin (albeit a partial one; Fig. 3*B*, lane 4). The diminished eplin phosphorylation did not arise from a reduction in ERK activity because the levels of active

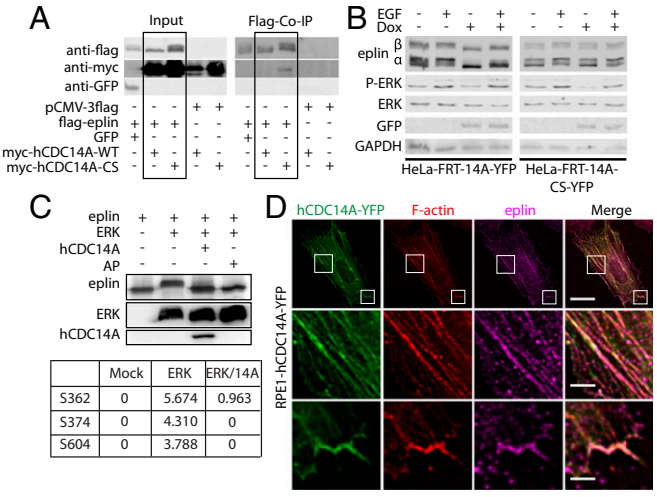

	Mock	ERK	ERK/14A
S362	0	5.674	0.963
S374	0	4.310	0
S604	0	3.788	0

Fig. 3. (*A*) Coimmunoprecipitation of flag-eplin and myc-hCDC14A in HEK293T cells. (*B*) Both isoforms of eplin showed upshift when the cells were treated with EGF. When the cells were simultaneously treated with doxycycline to induce *hCDC14A* expression, both isoforms of eplin migrated to an intermediate position. This was not seen in *hCDC14A*^{C278S}*-YFP* cells. (*C*) In vitro phosphatase assay. Eplin (lane 1) was first incubated with recombinant ERK (lane 2). The kinase reaction was stopped by addition of EDTA, and phosphorylated eplin was then incubated with either hCDC14A (lane 3) or alkaline phosphatase (lane 4). The table shows the phosphorylation intensity of the eplin residues (numbers refer to human β-eplin) as determined by mass spectrometry analysis. (*D*) Colocalization of hCDC14A-YFP and endogenous eplin at the cell leading edge and stress fibers. (Scale bars: *Upper* panel, 20 μm; *Middle* panel, 5 μm; *Lower* panel, 2.5 μm.) AP, alkaline phosphatase; Co-IP, coimmunoprecipitation; CS, change of Cys to Ser.

phosphorylated ERK that are universally used as indicators of ERK activity were unaffected by *hCDC14A* induction (Fig. 3*B*, P-ERK). As before, expression of *hCDC14*^{C278S} had no influence upon eplin phosphorylation by ERK (Fig. 3*B*, lane 8). We conclude that hCDC14A dephosphorylates eplin to counteract phosphorylation of eplin by ERK kinase.

Given this striking in vivo correlation between hCDC14A and dephosphorylation of the ERK target sites in both eplin isoforms, we assessed the ability of hCDC14A to directly dephosphorylate these residues in an in vitro phosphorylation/dephosphorylation assay. Because α-eplin was expressed to higher levels in *Escherichia coli* than β-eplin, we used this protein as the substrate for this assay (Fig. S3 *C*–*E*). Phosphorylation of recombinant α-eplin by human ERK1 kinase invoked an upshift of the α-eplin band in the SDS/PAGE (Fig. 3*C*, lane 2). Incubation with the nonspecific alkaline phosphatase triggered a downshift of this eplin back toward the position at which the initial recombinant, nonphosphorylated α-eplin migrated. Thus, the mobility shift of recombinant α-eplin was a consequence of direct phosphorylation by ERK1. Importantly, incubation of ERK1-phosphorylated α-eplin with recombinant hCDC14A induced an identical downshift of the α-eplin band (Fig. 3*C*). Mass spectrometry analysis showed that the serine residues 362, 374, and 604 of eplin were phosphorylated by ERK and subsequently dephosphorylated of recombinant hCDC14A (Fig. 3*C*). For unknown reasons, the peptide carrying S609 was not identified in three repeated mass spectrometry analyses. We conclude that hCDC14A has the ability to directly dephosphorylate the ERK1 kinase target phosphorylation sites of eplin.

Dephosphorylation of eplin by hCDC14A implies that both proteins colocalize in cells. Indeed, in RPE1 *hCDC14A-YFP* stable cells, endogenous eplin colocalized with hCDC14A-YFP at the cell edge and along stress fibers (Fig. 3*D*) to suggest that hCDC14A dephosphorylates eplin at these locations.

hCDC14A Regulates F-Actin Through Dephosphorylation of Eplin. The fact that eplin is an actin bundler (16) and the finding that eplin is an hCDC14A substrate (Fig. 3) raise the possibility that hCDC14A regulates actin dynamics through eplin. This model predicts that hCDC14A counteracts EGF-induced changes of the actin cytoskeleton. We tested this possibility by analyzing F-actin structures in HeLa Tet$_{ON}$-*hCDC14A* cells by combining EGF-induced eplin phosphorylation with Tet$_{ON}$-*hCDC14A* induction. EGF treatment of HeLa cells promoted the formation of large plasma membrane ruffles that are characterized by highly dynamic actin rearrangements in their lamellipodia (Fig. 4 *A* and *B*; EGF, Dox−) (31, 32). Dox-induced expression of *hCDC14A* inhibited this EGF-induced ruffling of the membranes (Fig. 4 *A* and *B*; EGF, Dox+) to suggest that hCDC14A can counteract EGF-induced changes of the actin cytoskeleton.

We next performed experiments designed to interrogate the role played by the EGF/hCDC14A control of eplin in this modulation of the F-actin cytoskeleton. HeLa cells were treated with or without EGF; cells were then transfected either with a mock control or *eplin-GFP* constructs alongside *myc-hCDC14A* as indicated. Overexpression of *eplin-GFP* induced the formation of robust stress fibers without the formation of lamellipodia (Fig. 4 *C*–*F*). Addition of EGF together with *eplin-GFP* expression promoted formation of lamellipodia and reduced the number of stress fibers (Fig. 4 *C*–*F*; compare eplin-GFP with EGF+eplin-GFP). These results are consistent with the previous observation that phosphorylation of eplin by ERK reduces its ability to bundle actin filaments (17). Consistently, expression of the phospho-inhibitory *eplin*$^{S362/S604A}$ promoted the generation of stress fiber but abolished lamellipodia formation even in the presence of EGF (Fig. 4 *C*–*E*). Thus, inhibition of stress fiber formation by EGF is mediated by ERK-induced phosphorylation of eplin. We also analyzed the impact of the additional phospho-sites in eplin (Fig. S4 *A*–*C*) and found that the inclusion of the phospho-blocking mutations S374A and S609A alongside

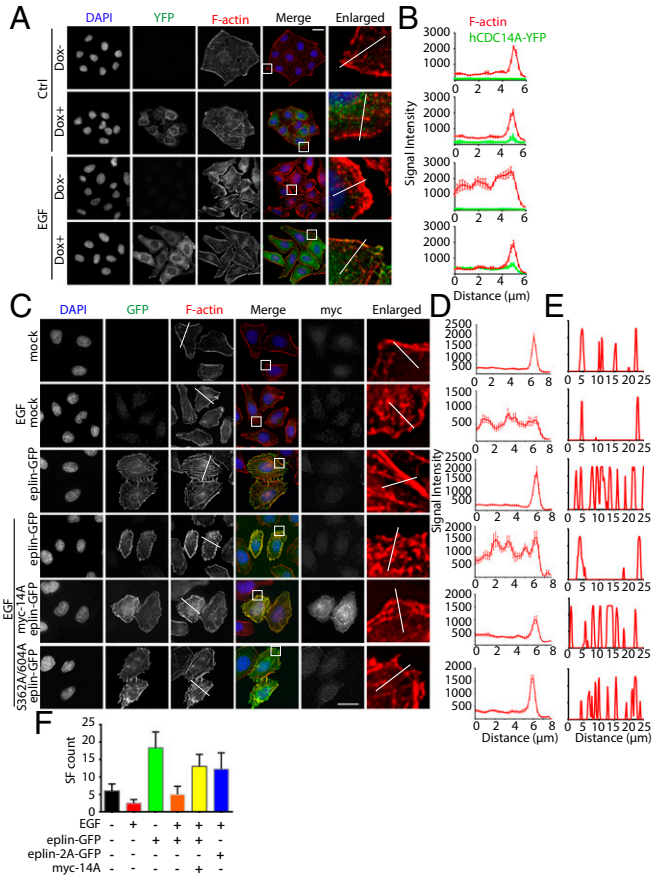

Fig. 4. (*A*) The formation of membrane ruffles was inhibited by ectopic *hCDC14A* expression. The "Enlarged" panel reflects a sevenfold magnification of the white boxed area in the "Merge." (Scale bar: 20 μm.) (*B*) Line scans of the cell edge (white lines in *A*). $n = 10$ regions of interest. Error bars: ± SEM. (*C*) Eplin bundled F-actin to thick stress fibers in HeLa cells. The "Enlarged" panel reflects a sevenfold magnification of the white boxed area in the "Merge." (Scale bar: 20 μm.) (*D*) Plot profiling of the F-actin fluorescence signal across the cell leading edge. The scan was along the white line in *C*, "Enlarged panel." $n = 10$ regions of interest. Error bars: ± SEM. (*E*) Plot profiling of stress fibers in the representative cell of *C*. After background subtraction, the scan was along the white line in *C*, "F-actin panel." (*F*) Quantification of stress fibers (SF) in cells of *C*. $n = 20$ cells. Error bars: ± SD. Ctrl, control.

S362A and S604A in the same molecule of eplin did not further influence the ability of eplin to induce stress fibers under EGF induction beyond the impact of the double S362A S604A change. Thus, phosphorylation of S362 and S604 alone is sufficient to inactivate the F-actin bundling activity of eplin. Finally, coexpression of *hCDC14A* and *eplin-GFP* in EGF-treated cells supported the formation of stress fibers and inhibited lamellipodia formation (Fig. 4 *C*–*F*). We conclude that hCDC14A counteracts ERK-induced inactivation of the bundling activity of eplin by directly dephosphorylating this key regulator of the F-actin cytoskeleton.

***hCDC14A*^{PD} and *eplin*^{KO} Cells Display a Reduction in E-Cadherin and a Decline in the Enrichment of β-Catenin at Cell–Cell Adhesion Sites.** Eplin links the E-cadherin–catenin complex to F-actin (23). Downregulation of eplin frequently occurs in cancer tissues and contributes to the epithelia-to-mesenchymal transition (EMT) that enhances cancer cell metastasis and chemo-resistance of tumors (23, 33–37).

To determine whether eplin regulation by hCDC14A and EGF contributes to EMT, we knocked out the *eplin* gene in human colon

cancer HCT116 cells using the CRISPR/Cas9 system (Fig. S2 *B–D*). Independent knockout clones were confirmed by sequencing of the chromosomal locus and immunoblot analysis with eplin antibodies (Fig. S2 *C* and *D*). Two independent *eplin*^{KO} clones, *eplin*^{KO}-23 and -33, showed an ∼50% reduction in E-cadherin protein levels (Fig. 5 *A* and *B*). The loss of linkage between the E-cadherin–catenin complex and F-actin has previously been shown to destabilize the E-cadherin protein at cell adhesion sites and promote a similar reduction in E-cadherin levels (38, 39). Furthermore, E-cadherin levels were also reduced in *hCDC14A*^{PD} (hCDC14A phosphatase dead version) cells (Fig. 5 *A* and *B*) that carried hyperphosphorylated, inactive eplin (Fig. 1). Thus, hCDC14A-mediated dephosphorylation of eplin plays an important role in stabilizing the molecular linkage of cell–cell adhesion. This notion was further supported by the observation that enrichment of β-catenin at cell–cell junctions in *hCDC14A*^{PD} and *eplin*^{KO} cells was decreased, even though total cellular β-catenin levels remained constant (Fig. 5 *A–D*).

To determine whether β-catenin mislocalization is a direct consequence of the hyper-phosphorylation of eplin, we expressed the *eplin*$^{S362/S604}$ phospho-mimetic and -inhibitory forms in *eplin*^{KO} and WT cells. Interestingly, eplin$^{S362A/S604A}$ restored the β-catenin organization as efficiently as WT eplin, yet eplin$^{S362D/S604D}$ failed to do so (Fig. 5 *E* and *F*). This result suggests that phosphorylation of eplin at S362 and S604 regulates recruitment of β-catenin to cell adherens sites.

The β-catenin/E-cadherin phenotype of *hCDC14A*^{PD} and *eplin*^{KO} cells suggests that both hCDC14A and eplin stabilize the E-cadherin–α/β-catenin complex. Consequently, it can be anticipated that malfunction of either hCDC14A or eplin may eventually affect cell–cell adhesion and promote metastasis. We therefore used a soft agar tumor formation assay as a test of this hypothesis. Both HCT116 *hCDC14A*^{PD} and *eplin*^{KO} cells formed tumor colonies with rough edges, whereas WT cells formed compact colonies with smooth edges (Fig. 5 *G* and *H*). In fact, both *hCDC14A* and *eplin* are significantly down-regulated in colorectal carcinoma (Fig. 5*I*) (20). This down-regulation is associated with poor survival in cancer patients (Fig. 5*J*) (20). Taken together, we suggest that hCDC14A regulates cell migration and adhesion through dephosphorylation of eplin (Fig. 5*K*).

Discussion

We have previously shown that human CDC14A regulates cell migration and cell adhesion (20). One of the major bottlenecks for understanding the phenotypes arising from manipulation of CDC14A in functional studies of human CDC14 phosphatases has been the lack of a defined cohort of substrates. We have therefore combined phospho-proteomics and BioID analyses to generate a comprehensive list of the components of the molecular network regulated by hCDC14A. The actin regulator eplin occupies a pivotal position within this network (Figs. 1, 2, and 5*K*). It is well known that phosphorylation of eplin by ERK at S362 and S604 decreases its actin-bundling affinity (17). Strikingly, we find that dephosphorylation of these sites by hCDC14A regulates the balance between formation of stress fibers and membrane ruffling that is promoted by EGF stimulation (Fig. 4).

Eplin provides the molecular linkage between the actin cytoskeleton and the E-cadherin–catenin complex that is critical for stabilizing cell–cell adhesion and maintaining apical cell polarity (23) (Fig. 5). We recorded a reduction in β-catenin enrichment at cell–cell junctions in both *eplin*^{KO} and *hCDC14A*^{PD} cells to indicate that the dephosphorylation of eplin by hCDC14A is required to stabilize this interaction (Fig. 5*K*). Moreover, the protein level of E-cadherin was significantly reduced in both cell lines, probably due to the destabilization of the E-cadherin–α/β-catenin–F-actin association (Fig. 5). Because of the prominent roles that E-cadherin plays in maintaining proper cell–cell adhesion, polarity of epithelial cells, and sequestration of the oncoprotein β-catenin at the plasma membrane, down-regulation of E-cadherin is a frequent event during carcinogenesis (40–44). Loss of E-cadherin often leads to EMT and enhanced invasion and metastasis. This may explain why the *eplin*^{KO} and *hCDC14A*^{PD} colonies in soft agar have rough edges (Fig. 5*G*) (20). Importantly, a reduction of hCDC14A and eplin levels is frequently observed in colorectal carcinoma and is associated with poor prognosis

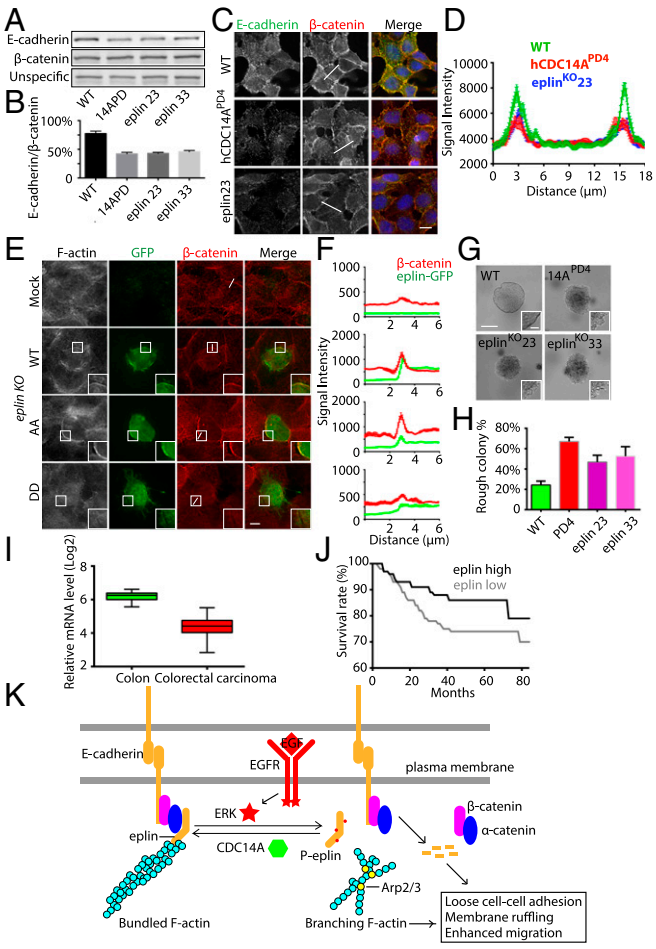

Fig. 5. (*A*) Immunoblot of E-cadherin/β-catenin in HCT116 WT cells, hCDC14A^{PD}, and the two eplin^{KO} clones. (*B*) Quantification of the E-cadherin/β-catenin ratio from *A*. $n = 3$ independent experiments. Error bars: ± SD. (*C*) β-Catenin enrichment at cell–cell junction was reduced in *hCDC14A*^{PD} and *eplin*^{KO} cells compared with WT cells. (Scale bar: 10 μm.) (*D*) Quantification of β-catenin signal at cell–cell junction in *C*. Line scan across the individual cell was used to profile the signal distribution of β-catenin (white lines in *C*). The two peaks represent the β-catenin enrichment at the cell–cell junction. $n = 20$ regions of interest. Error bars: ± SEM. (*E*) HCT116 *eplin*^{KO} cells were transfected with the indicated *eplin-GFP* constructs. Fixed cells were analyzed. (Scale bar: 2 μm.) The white box on the right side of each panel is a twofold enlargement of the smaller boxed area. (*F*) Line scans along the white lines in the β-catenin (*E*). $n = 10$ regions of interest. Error bars: ± SEM. (*G*) Soft agar colony assay of the indicated HCT116 clonal cell lines. (*H*) Quantification of *G*. Number of rough colonies was determined. $n = 30$. Error bars: ± SD. (Scale bars: 300 μm; *Inset*, 20 μm.) (*I*) Eplin mRNA was significantly down-regulated in colorectal carcinoma compared with healthy colon. Data were extracted from the Oncomine database (https://www.oncomine.org/index.jsp). ($n = 12$, colon; 68, colorectal carcinoma). Bars: The whiskers go down to the smallest value and up to the largest, respectively. (*J*) Poor prognosis of colon cancer patients was correlated with a low level of eplin expression. Kaplan–Meier survival data were obtained from R2: Genomics Analysis and Visualization Platform (https://hgserver1.amc.nl/cgi-bin/r2/main.cgi). (n = high, 74; low, 204). (*K*) Model for the regulation of eplin by ERK and hCDC14A. AA, eplin S362A/S604A; DD, eplin S362D/S604D.

in cancer patients (Fig. 5 *I* and *J*) (20, 34, 35). Collectively, we propose that the balance of eplin phosphorylation that is maintained by the antagonistic activities of ERK and hCDC14A toward conserved phosphorylation sites on eplin plays a key role in regulating actin dynamics to modulate cell migration and adhesion of both normal and transformed cells (Fig. 5*K*). Thus, hCDC14A and eplin are important factors in restraining tumor aggressiveness.

Materials and Methods

Cell Culture. HeLa FRT and HEK 293T cell lines were cultured in DMEM GlutaMax medium containing 10% FBS, 100 units/mL penicillin, and 100 mg/mL streptomycin at 37 °C and 5% CO_2. Stable cell lines were constructed as previously described (20).

Quantitative Phospho-Proteomic Analysis. HeLa FRT YFP and hCDC14A-YFP cells were cultured in light and heavy SILAC medium, respectively. Proteins were extracted and mixed at a ratio of 1:1. Phospho-peptides were enriched as described (45). Peptide identification and quantification was achieved using the MaxQuant software package (1.5.3.8) (46). Results were analyzed using Perseus (47).

CRISPR/Cas9-Mediated Eplin Knockout. Guide RNA (gRNA) targeting the exon 9 of eplin was designed using a web tool (crispr.mit.edu/) (48). The transfected cells were sorted via FACS and seeded on 96-well plates for single-clone selection. The clones were harvested and screened via genomic PCR and Western blot.

Details are in *SI Materials and Methods* including experimental procedures and reagents.

No human or animal clinical experiment was done and no ethics approval was needed for the study.

ACKNOWLEDGMENTS. E.S. is supported by Deutsche Forschungsgemeinschaft Grant DFG Schi 295/3-3. T.R. is supported by Collaborative Research Centre Grant SFB1036.

1. Blanchoin L, Boujemaa-Paterski R, Sykes C, Plastino J (2014) Actin dynamics, architecture, and mechanics in cell motility. *Physiol Rev* 94:235–263.
2. Tojkander S, Gateva G, Lappalainen P (2012) Actin stress fibers: Assembly, dynamics and biological roles. *J Cell Sci* 125:1855–1864.
3. Ridley AJ (2011) Life at the leading edge. *Cell* 145:1012–1022.
4. Stevenson RP, Veltman D, Machesky LM (2012) Actin-bundling proteins in cancer progression at a glance. *J Cell Sci* 125:1073–1079.
5. Rognoni E, Ruppert R, Fässler R (2016) The kindlin family: Functions, signaling properties and implications for human disease. *J Cell Sci* 129:17–27.
6. Zhou Y, Su J, Shi L, Liao Q, Su Q (2013) DADS downregulates the Rac1-ROCK1/PAK1-LIMK1-ADF/cofilin signaling pathway, inhibiting cell migration and invasion. *Oncol Rep* 29:605–612.
7. Hall A (2012) Rho family GTPases. *Biochem Soc Trans* 40:1378–1382.
8. Sit ST, Manser E (2011) Rho GTPases and their role in organizing the actin cytoskeleton. *J Cell Sci* 124:679–683.
9. Siripala AD, Welch MD (2007) SnapShot: Actin regulators I. *Cell* 128:626.
10. Siripala AD, Welch MD (2007) SnapShot: Actin regulators II. *Cell* 128:1014.
11. Franzot G, Sjöblom B, Gautel M, Djinović Carugo K (2005) The crystal structure of the actin binding domain from alpha-actinin in its closed conformation: Structural insight into phospholipid regulation of alpha-actinin. *J Mol Biol* 348:151–165.
12. Meyer RK, Aebi U (1990) Bundling of actin filaments by alpha-actinin depends on its molecular length. *J Cell Biol* 110:2013–2024.
13. Yamashiro S, Yamakita Y, Ono S, Matsumura F (1998) Fascin, an actin-bundling protein, induces membrane protrusions and increases cell motility of epithelial cells. *Mol Biol Cell* 9:993–1006.
14. Delorme V, et al. (2007) Cofilin activity downstream of Pak1 regulates cell protrusion efficiency by organizing lamellipodium and lamella actin networks. *Dev Cell* 13:646–662.
15. Sumi T, Matsumoto K, Takai Y, Nakamura T (1999) Cofilin phosphorylation and actin cytoskeletal dynamics regulated by rho- and Cdc42-activated LIM-kinase 2. *J Cell Biol* 147:1519–1532.
16. Maul RS, et al. (2003) EPLIN regulates actin dynamics by cross-linking and stabilizing filaments. *J Cell Biol* 160:399–407.
17. Han MY, Kosako H, Watanabe T, Hattori S (2007) Extracellular signal-regulated kinase/mitogen-activated protein kinase regulates actin organization and cell motility by phosphorylating the actin cross-linking protein EPLIN. *Mol Cell Biol* 27:8190–8204.
18. Mocciaro A, Schiebel E (2010) Cdc14: A highly conserved family of phosphatases with non-conserved functions? *J Cell Sci* 123:2867–2876.
19. Visintin R, et al. (1998) The phosphatase Cdc14 triggers mitotic exit by reversal of Cdk-dependent phosphorylation. *Mol Cell* 2:709–718.
20. Chen NP, Uddin B, Voit R, Schiebel E (2016) Human phosphatase CDC14A is recruited to the cell leading edge to regulate cell migration and adhesion. *Proc Natl Acad Sci USA* 113:990–995.
21. Ji M, et al. (2012) Phospho-regulation of KIBRA by CDK1 and CDC14 phosphatase controls cell-cycle progression. *Biochem J* 447:93–102.
22. Roux KJ, Kim DI, Raida M, Burke B (2012) A promiscuous biotin ligase fusion protein identifies proximal and interacting proteins in mammalian cells. *J Cell Biol* 196:801–810.
23. Abe K, Takeichi M (2008) EPLIN mediates linkage of the cadherin catenin complex to F-actin and stabilizes the circumferential actin belt. *Proc Natl Acad Sci USA* 105:13–19.
24. Bremmer SC, et al. (2012) Cdc14 phosphatases preferentially dephosphorylate a subset of cyclin-dependent kinase (Cdk) sites containing phosphoserine. *J Biol Chem* 287:1662–1669.
25. Eissler CL, et al. (2014) The Cdk/cDc14 module controls activation of the Yen1 Holliday junction resolvase to promote genome stability. *Mol Cell* 54:80–93.
26. Gray CH, Good VM, Tonks NK, Barford D (2003) The structure of the cell cycle protein Cdc14 reveals a proline-directed protein phosphatase. *EMBO J* 22:3524–3535.
27. Lanzetti L, et al. (2007) Regulation of the Rab5 GTPase-activating protein RN-tre by the dual specificity phosphatase Cdc14A in human cells. *J Biol Chem* 282:15258–15270.
28. Tumurbaatar I, Cizmecioglu O, Hoffmann I, Grummt I, Voit R (2011) Human Cdc14B promotes progression through mitosis by dephosphorylating Cdc25 and regulating Cdk1/cyclin B activity. *PLoS One* 6:e14711.
29. Chen S, Maul RS, Kim HR, Chang DD (2000) Characterization of the human EPLIN (Epithelial Protein Lost in Neoplasm) gene reveals distinct promoters for the two EPLIN isoforms. *Gene* 248:69–76.
30. Zhang S, et al. (2013) Epidermal growth factor promotes protein degradation of epithelial protein lost in neoplasm (EPLIN), a putative metastasis suppressor, during epithelial-mesenchymal transition. *J Biol Chem* 288:1469–1479.
31. Isogai T, et al. (2015) Initiation of lamellipodia and ruffles involves cooperation between mDia1 and the Arp2/3 complex. *J Cell Sci* 128:3796–3810.
32. Balaji K, et al. (2012) RIN1 orchestrates the activation of RAB5 GTPases and ABL tyrosine kinases to determine the fate of EGFR. *J Cell Sci* 125:5887–5896.
33. Liu R, et al. (2016) Epithelial protein lost in neoplasm-α (EPLIN-α) is a potential prognostic marker for the progression of epithelial ovarian cancer. *Int J Oncol* 48:2488–2496.
34. Collins RJ, Jiang WG, Hargest R, Mason MD, Sanders AJ (2015) EPLIN: A fundamental actin regulator in cancer metastasis? *Cancer Metastasis Rev* 34:753–764.
35. Zhang S, et al. (2011) EPLIN downregulation promotes epithelial-mesenchymal transition in prostate cancer cells and correlates with clinical lymph node metastasis. *Oncogene* 30:4941–4952.
36. Ohoka A, et al. (2015) EPLIN is a crucial regulator for extrusion of RasV12-transformed cells. *J Cell Sci* 128:781–789.
37. Steder M, et al. (2013) DNp73 exerts function in metastasis initiation by disconnecting the inhibitory role of EPLIN on IGF1R-AKT/STAT3 signaling. *Cancer Cell* 24:512–527.
38. Le TL, Yap AS, Stow JL (1999) Recycling of E-cadherin: A potential mechanism for regulating cadherin dynamics. *J Cell Biol* 146:219–232.
39. Kowalczyk AP, Nanes BA (2012) Adherens junction turnover: Regulating adhesion through cadherin endocytosis, degradation, and recycling. *Subcell Biochem* 60:197–222.
40. Martin-Belmonte F, Perez-Moreno M (2011) Epithelial cell polarity, stem cells and cancer. *Nat Rev Cancer* 12:23–38.
41. Moreno-Bueno G, Portillo F, Cano A (2008) Transcriptional regulation of cell polarity in EMT and cancer. *Oncogene* 27:6958–6969.
42. Umbas R, et al. (1992) Expression of the cellular adhesion molecule E-cadherin is reduced or absent in high-grade prostate cancer. *Cancer Res* 52:5104–5109.
43. Berx G, Van Roy F (2001) The E-cadherin/catenin complex: An important gatekeeper in breast cancer tumorigenesis and malignant progression. *Breast Cancer Res* 3:289–293.
44. Oka H, et al. (1993) Expression of E-cadherin cell adhesion molecules in human breast cancer tissues and its relationship to metastasis. *Cancer Res* 53:1696–1701.
45. Villén J, Gygi SP (2008) The SCX/IMAC enrichment approach for global phosphorylation analysis by mass spectrometry. *Nat Protoc* 3:1630–1638.
46. Cox J, Mann M (2008) MaxQuant enables high peptide identification rates, individualized p.p.b.-range mass accuracies and proteome-wide protein quantification. *Nat Biotechnol* 26:1367–1372.
47. Tyanova S, et al. (2016) The Perseus computational platform for comprehensive analysis of (prote)omics data. *Nat Methods* 13:731–740.
48. Hsu PD, et al. (2013) DNA targeting specificity of RNA-guided Cas9 nucleases. *Nat Biotechnol* 31:827–832.